

UKAEA FUS 543

J.W. Connor, T.J. Martin

Rotation shear and drift wave stability

Enquiries about copyright and reproduction should in the first instance be addressed to the Culham Publications Officer, Culham Centre for Fusion Energy (CCFE), Library, Culham Science Centre, Abingdon, Oxfordshire, OX14 3DB, UK. The United Kingdom Atomic Energy Authority is the copyright holder.

Rotation shear and drift wave stability

J.W. Connor, T.J. Martin

EURATOM/UKAEA Fusion Association, Culham Science Centre, OX14 3DB, Abingdon, UK

UKAEA FUS 543

EURATOM/UKAEA Fusion

Rotation Shear and Drift Wave Stability

JW Connor and TJ Martin

April 2007

© UKAEA

EURATOM/UKAEA Fusion Association

Culham Science Centre
Abingdon
Oxfordshire
OX14 3DB
United Kingdom

Telephone: +44 1235 466586

Facsimile: +44 1235 466435

UKAEA



Rotation Shear and Drift Wave Stability

J W Connor and T J Martin

EURATOM/UKAEA Fusion Association, Culham Science Centre, Abingdon,
Oxon OX14 3DB, UK

Abstract

The stability of short wave-length drift instabilities in toroidally confined plasma is conventionally analysed using the ballooning transformation. This reduces the two-dimensional stability problem to the solution of two consecutive one-dimensional equations. The first, the lowest order in n (n is the toroidal mode number), equation produces a local eigenvalue that is a function of radius, x , due to profile variation and also has a periodic dependence on a parameter k , representing a radial wave-number. Usually one finds that profile variation defines a radial position where the growth rate is a maximum. In next order one finds that this position determines the mode's radial location and that the parameter k is such as to maximise the growth rate. However, if the effects of sheared plasma rotation, $d\Omega/dq$, dominate other profile variation, one finds the growth rate is smaller and, instead, involves an average over a period of k . This is a reversion to an essentially cylindrical situation, where toroidal coupling effects between adjacent resonant surfaces are eliminated. In this paper we consider a generic drift wave model that generates a local eigenvalue having quadratic radial variation of frequency, ω , and growth rate, γ , and periodic variation with k . We derive an analytic dispersion relation. Although requiring numerical solution, this shows there is a continuous evolution between these two limits as $d\Omega/dq$ increases, the transition being quite sharp for high n . The transition can be associated with a critical rotation shear, $d\Omega^{\text{crit}}/dq \sim O(1/n)$. The detailed character of the results depends on which of the radial variations, $\omega(x)$ or $\gamma(x)$, dominates. Numerical solutions concentrate on three significant cases: (i) a radial variation just in the growth rate; (ii) a radial variation just in the real frequency; and (iii) comparable radial variations in both. The results are complex to summarise, particularly as to which conventional mode links to which mode in the rotation dominated case, and one must consider each case in detail. However one can conclude in general that the most unstable modes do correspond to an average over k of the conventional ballooning mode and are hence more stable, thus reducing transport. Since case (i) is isomorphic to the ideal MHD stability problem (in the absence of stable values of k when there is an associated MHD continuum), one can immediately deduce that rotation shear then also reduces the growth rate of pressure gradient driven ballooning modes by averaging over k .

1 Introduction

Anomalous plasma transport in magnetic confinement devices, such as tokamaks, is believed to be caused by micro-instabilities of drift wave character, e.g. trapped electron modes and ion and electron temperature gradient instabilities (i.e. ITG and ETG modes respectively). The ballooning transformation [1 - 4] provides a method for calculating the eigenfunctions and stability of perturbations with such short wavelength (high toroidal mode number, n) in a torus. This approach allows one to simplify the problem by introducing an eikonal representation for the perturbation at high n .

The ballooning representation overcomes the conflict that then arises in the presence of magnetic shear between the requirements of long wavelength along the magnetic field, characteristic of the most unstable modes, and the double periodicity in a torus. It reduces the apparently two-dimensional stability problem to one involving the solution of two consecutive one-dimensional equations, a major simplification. The first, the lowest order

in n equation, is an equation along the magnetic field line, i.e. in a ‘poloidal’ angle. However this poloidal angle θ covers an infinite range, rather than the 2π period of the equilibrium poloidal angle θ . It produces a ‘local’ eigenvalue, $\omega(x, k) = \omega(x, k)$ [5, 6, 7] that is a function of radius, x , due to profile variation and also has a periodic dependence on a parameter k that can be interpreted as a radial wave-number. In next order one uses this local eigenvalue in a WKB phase integral for $k(x, \theta)$ to determine the global eigenvalue, ω , and the radial structure, $k(x)$. One finds that the mode’s radial location and the parameter k are both determined so as to maximise the local growth rate, $\gamma(x, k)$.

This method has been applied to a number of instabilities and provides a complete theory - provided magnetic shear, $s = (r/q)(dq/dr) = rq'/q$ (where q is the safety factor and prime denotes a derivative with respect to minor radius, r), is not too low and that rotation shear, dO/dq , is sufficiently weak. Unfortunately these conditions are not well met in the vicinity of transport barriers; the micro-stability of such barriers is a topic of considerable interest. In this paper we consider the effect of rotation shear, assuming its effect can be represented as a Doppler shift to the mode frequency.

It is possible to consider the effect of rotation shear on stability using the wave-number representation [5, 8 - 10], which is equivalent to the ballooning representation, but more convenient, for analysing such cases. One again needs to solve the lowest order ballooning equation in θ , but there is also an eikonal factor with a fast, $O(n)$, dependence on k . The eigenvalue condition is to ensure that this function is periodic in k for the physical perturbation to be periodic in θ . In this approach one finds that, in the limit where the sheared rotation dominates the effects of other profile variations, the growth rate is reduced, being given by its average over the periodic parameter k , i.e. $\omega = \langle \gamma(k) \rangle$ [7, 11, 12]. This raises the question as to whether this mode arises as a continuous evolution of the conventional ballooning mode as dO/dq increases.

This matter can be explored with the wave-number representation by simultaneously including the effects of profile variation and rotation shear. With a quadratic radial variation and a sinusoidal dependence of $\omega(k)$ on k , this requires the solution of a Mathieu equation in k . Floquet solutions of this equation can satisfy the appropriate periodicity condition on k . The method has been applied to high- n ideal MHD ballooning modes [13] and by Dewar to a particular, simple model possessing the features of an electrostatic drift wave that has a similar structure to the MHD problem [10]. The model in Ref. 10 assumes that the profile variation affects only the growth rate. An important outcome of these calculations is that for high values of n there is a sharp, but continuous, transition from the conventional ballooning mode to the rotation dominated one as dO/dq increases. The transition determines a critical value: $(dO/dq)^{\text{crit}} \sim O(1/n)$. This means that the conventional high- n mode is not robust to a modest level of rotation shear.

In this paper we consider the case where profile variation also affects the real frequency, e.g. through the variation of the diamagnetic frequency, $\omega_{*e} = (nq/r)(T_e/eBL_n)$, where T_e is the electron temperature, e the electronic charge, B the magnetic field and L_n a density scalelength. As we will show, the relative strengths of these two variations, $\omega(x)$ and $\gamma(x)$, play a key role in determining the nature of the solutions.

2. The Wave-number Representation and the Drift Wave Model

The wave-number representation expresses the perturbed electrostatic potential, $f(\theta, x)$, where we Fourier analyse in the toroidal angle, $f \sim \exp(in\theta)$, in the form [5, 10]:

$$\varphi(\theta, x) = \int_{-\infty}^{\infty} dk \hat{\varphi}(\theta, k) \exp[-inq'x(\theta - k) + inq'S(k)] \quad (1)$$

Here the radial co-ordinate, x , is measure from some reference resonant surface where $nq(r) = m_0$, an integer. The function $\hat{\varphi}(\theta, k)$ satisfies the lowest order ballooning equation on the interval $-\infty < \theta < \infty$:

$$L(\theta, k; x) \hat{\varphi}(\theta, k; x) = \lambda(k, x) \hat{\varphi}(\theta, k; x) \quad (2)$$

where the operator $L(\theta, k)$ has the property that the solution of eqn. (2) satisfies the condition $\hat{\varphi}(\theta + 2\pi, k + 2\pi) = \hat{\varphi}(\theta, k)$. As a consequence, $S(k)$ must be a periodic function of k on the interval 2π to ensure that $f(\theta, x)$ is periodic in θ . This provides the global eigenvalue condition.

Introducing the form (1) leads to the substitution [7]

$$x \rightarrow -dS/dk \quad (3)$$

in eqn. (2), so that

$$\lambda = \lambda(k, -dS/dk) \quad (4)$$

The toroidal plasma rotation, O , is introduced through a Doppler shift

$$\omega \rightarrow \omega - n\Omega(x) \quad (5)$$

so that for constant rotation shear, eqn. (4) is replaced by

$$\lambda + nq'(dO/dq)(dS/dk) = \lambda(k, -dS/dk) \quad (6)$$

Let us introduce a generic drift wave model for $\lambda(x, k)$, namely

$$\lambda(x, k) = \lambda_0 - \lambda_1 x^2/L_e^2 + i\lambda_2 - i\lambda_3 x^2/L_e^2 + e^{-\lambda_4} \cos k \quad (7)$$

which represents radial expansions about co-incident maxima in both λ_0 and λ_2 , each of which might peak at the steepest radial profile gradient, say through $\lambda_{*e} = (nq/r)(T_e/eBL_n)$ or $\lambda_{*i}^T = (nq/r)(T_i/eBL_{Ti})$, where L_{Ti} is the ion temperature scalelength. The particular periodic dependence in k shown in eqn. (7) can be readily generalised, as we shall see

below. The parameter ϵ , representing toroidal coupling, can be complex and $O(1)$ in general. Then eqns. (6) and (7) imply

$$\begin{aligned} \psi + nq'(dO/dq)(dS/dk) = \psi_0 - (\gamma_1/L\gamma^2)(dS/dk)^2 \\ + i\gamma_1 - i(\gamma_2/L\gamma^2)(dS/dk)^2 + \epsilon \psi_0 \cos k \end{aligned} \quad (8)$$

It is convenient to introduce $\psi = \exp(inq'S)$ so that eqn.(8) is replaced by:

$$\left[\frac{1}{\Lambda^4} \frac{d^2}{dk^2} + \hat{\Omega}_q \frac{d}{dk} + \left(\frac{\gamma_0}{\omega_0} - \frac{i(\omega_0 - \omega)}{\omega_0} + \hat{\epsilon} \cos k \right) \right] \psi = 0 \quad (9)$$

where

$$\Lambda^{-4} = \left[\frac{\gamma_1}{\omega_0(nq'L_\gamma)^2} - i \frac{\omega_1}{\omega_0(nq'L_\omega)^2} \right], \quad \hat{\Omega}_q = \frac{\Omega_q}{\omega_0}, \quad \hat{\epsilon} = -i\epsilon \quad (10)$$

It is also convenient to write:

$$\psi^2 = \psi_0^2 \exp(-ia), \quad \hat{\epsilon} = \hat{\epsilon}_0 \exp(i\delta) \quad (11)$$

where ψ_0 , $\hat{\epsilon}_0$, a and δ are all real and $\psi_0 \gg 1$. A further substitution, $\psi \rightarrow \xi \exp(-\Lambda^4 \hat{\Omega}_q k/2)$, reduces this to a Mathieu equation [14]:

$$\left[\frac{1}{\Lambda^4} \frac{d^2}{dk^2} + \left(\frac{\gamma_0}{\omega_0} - \frac{i(\omega_0 - \omega)}{\omega_0} - \left(\frac{\Lambda^2 \hat{\Omega}_q}{2} \right)^2 + \hat{\epsilon} \cos k \right) \right] \xi = 0 \quad (12)$$

where periodicity of ψ implies ξ must be a Floquet solution satisfying [14, 15]

$$\xi(2\pi) = \cosh(\Lambda^4 \hat{\Omega}_q \pi) \xi(0) \quad (13)$$

Finally, it is convenient to write eqn. (12) in the form:

$$\left[\frac{1}{\Lambda^4} \frac{d^2}{dk^2} + 2\hat{\epsilon} \left(\frac{\sigma}{\Lambda^2 (2\hat{\epsilon})^{1/2}} - \sin^2 \left(\frac{k}{2} \right) \right) \right] \xi = 0 \quad (14)$$

where

$$\frac{(\gamma - i\omega)}{\omega_0} = \left[\frac{\gamma_0}{\omega_0} - i - \left(\frac{\Lambda^2 \hat{\Omega}_q}{2} \right)^2 + \hat{\epsilon} - \frac{(2\hat{\epsilon})^{1/2} \sigma}{\Lambda^2} \right] \quad (15)$$

Equation (14) is of Schrödinger type with potential $Q(k)$ where:

$$Q(k) = -2\hat{\epsilon}\Lambda^4 \left(\frac{\sigma}{\Lambda^2 (2\hat{\epsilon})^{1/2}} - \sin^2 \left(\frac{k}{2} \right) \right) \quad (16)$$

Thus the eigenvalue problem is to determine the value of s that ensures $\psi(k)$ satisfies the periodicity condition, eqn. (13), where we take $\psi = 1$ and $(d\psi/dk) = 0$ at $k = 0$. Then one can calculate ω and γ from eqn. (15).

3 Solution of the Eigenvalue Problem

We can exploit the large parameter ω_0 to obtain solutions to eqn. (14) in the WKB approximation [16]:

$$\xi_{\pm}(k) \sim Q^{-1/4} \exp \left(\pm i \int^k Q^{1/2}(k) dk \right) \quad (17)$$

It is then important to identify the turning points where $Q(k) = 0$ and the associated anti-Stokes lines where $\text{Im} Q(k) = 0$. If the anti-Stokes lines do not intercept the real k - axis on a 2π interval, a solution satisfying the appropriate boundary conditions is

$$\xi(k) = Q^{-1/4} \cosh \left(\int_0^k Q^{1/2}(k) dk \right) \quad (18)$$

In this case, the eigenvalue condition (13) is simply

$$\Lambda^4 \hat{\Omega}_q \pi = \int_0^{2\pi} Q^{1/2}(k) dk - 2\pi i \ell \quad (19)$$

where ℓ is an integer. Clearly $\hat{\Omega}_q$ must be sufficiently large for the two sides of eqn. (19) to balance, i.e. $\hat{\Omega}_q \sim 1/\omega_0^2$. These solutions correspond to the ‘passing’ or ‘open’ orbits in a WKB analysis, when the eigenvalue is determined by an average over k [8, 10, 17], as indicated by eqn. (19).

If the anti-Stokes lines do intersect the k -axis on $(0, 2\pi)$ a WKB analysis leads to the result (see eqn. (A.15) in Appendix A and Ref. 15):

$$\cosh\left(\Lambda^4 \hat{\Omega}_q \pi\right) = \left[\exp\left(\int_I Q^{1/2}(k) dk\right) + \frac{1}{4} \exp\left(-\int_I Q^{1/2}(k) dk\right) \right] \cos\left(\int_{II} Q^{1/2}(k) dk\right) \quad (20)$$

where we have again used eqn. (13). Here the interval II is between turning points (k_1, k_2), so the argument of the ‘cosine term’ is real and I is the sum of the intervals $(0, k_1)$ and $(k_2, 2p)$. Since the ‘exponential term’ is exponentially large, the only way eqn. (20) can be satisfied is by ensuring that $\int_{II} Q^{1/2}(k) dk \approx 0$; this determines a set of pairs of turning points and associated eigenvalues, s , corresponding to the energy levels in the ‘potential’ $Q(k)$, a standard WKB problem. The turning points for the lowest energy levels are close together and one can introduce a quadratic expansion of $Q(k)$ about $k = 0$. In Appendix B we show how, by expanding in $k \sim \left|2(2\hat{\epsilon})^{-1/4} (\sigma/\Lambda^2)^{1/2}\right| \ll 1$, one can derive an analytic expression for $\xi(2\pi)$ to be used in eqn. (13). This determines the eigenvalue σ , and allows one to span the transition from the ‘localised’, or ‘bound state’, solutions to the ‘passing’ limit (19) as $\hat{\Omega}_q$ increases.

The outcome (see eqn. (B.23) in Appendix B and Langer [15]) is a calculation of $\xi(2\pi)$ to insert in eqn. (13), leading to a dispersion relation for $\sigma(\hat{\Omega}_q)$. Thus we obtain:

$$\cosh\left(\Lambda^4 \hat{\Omega}_q \pi\right) = \frac{1}{(2\pi)^{1/2}} \frac{\exp\left(4\Lambda^2 (2\hat{\epsilon})^{1/2}\right)}{\left(16\Lambda^2 (2\hat{\epsilon})^{1/2}\right)^\sigma} \cos(\pi\sigma) \Gamma\left(\frac{1}{2} + \sigma\right), \quad \text{Re } \sigma > 0 \quad (21)$$

As noted in Appendix B, eqn. (B.24), this result can be generalised to a more complex poloidal variation, $f(k)$, than a single harmonic with a simple correspondence in eqn. (21), $\hat{\epsilon} \rightarrow f''(0)$. At the same time the full form of $f(k)$ appears in eqn. (19) and the term linear in $\hat{\epsilon}$ on the right hand side of eqn. (15) is replaced by $f(0)$.

Using Stirling’s Formula for the asymptotic forms of the Gamma functions at large s [18] and the Reflection Formula, one finds the result (21) smoothly match onto eqns. (18) and (20) in the appropriate limits. The zeros of $\cos s$ in eqn. (21) at $s = p+1/2$, with p an integer, correspond to the bound state solutions for small $\hat{\Omega}_q$. These are the conventional ballooning mode and its harmonics. In the next section we explore solutions of the dispersion relation for s as a function of $\hat{\Omega}_q$ and its implications for ξ and η through eqn. (15).

For larger positive values of s (or p), the turning points become widely separated, corresponding to ‘energy levels’ nearer the top of the potential well given by $Q(k)$. In this case the approximation underlying eqns. (21) breaks down. In general one can use a WKB phase-integral analysis [16] to determine the eigenvalues s for these higher

harmonics of the conventional ballooning mode. However, to explore the effect of $\hat{\Omega}_q$ on these higher harmonics, one can derive a complementary result to eqn. (21) for the case when the turning points both lie close to $k = p$. Introducing a quantity $\hat{\sigma} = \sigma - (2\hat{\epsilon})^{1/2} \Lambda^2$, we derive in Appendix C, see eqn. (C.23), a corresponding equation for $\gamma(2p)$ for substituting into eqn. (13):

$$\begin{aligned} \cosh\left(\Lambda^4 \hat{\Omega}_q \pi\right) &= \sqrt{\frac{\pi}{2}} \frac{\exp\left(\frac{4i\sqrt{2\hat{\epsilon}} \Lambda^2 - \hat{\sigma}\pi}{2}\right)}{\Gamma(1/2 + i\hat{\sigma})} (16\sqrt{2\hat{\epsilon}} \Lambda^2)^{i\hat{\sigma}} \\ &+ \frac{\Gamma(1/2 + i\hat{\sigma})}{\sqrt{2\pi}} \cosh(\hat{\sigma}\pi) \exp\left(\frac{-4i\sqrt{2\hat{\epsilon}} \Lambda^2 - \hat{\sigma}\pi}{2}\right) (16\sqrt{2\hat{\epsilon}} \Lambda^2)^{-i\hat{\sigma}} \end{aligned} \quad (22)$$

A more symmetric form is given in Appendix C, eqn. (C.24), which emphasizes the fact that for real Λ_0^2 , $\hat{\epsilon}$ and $\hat{\sigma}$ this equation is purely real. Indeed in this case it reduces to a result of Langer [15], where we recall $\hat{\sigma} = \sigma - \sqrt{2\hat{\epsilon}} \Lambda^2$. Introducing this replacement into eqn. (15) for the frequency and growth rate is equivalent to the substitution $\sigma \rightarrow \hat{\sigma} \hat{\epsilon} \rightarrow -\hat{\epsilon}$. Again using Stirling's Formula for the asymptotic forms of the Gamma functions at large s [20], one finds the result (22) smoothly matches to eqns. (18) and (20) in the appropriate limits.

4 Results for $\gamma(\hat{\Omega}_q)$ and $\gamma(\hat{\Omega}_q)$

In this section we explore the impact of rotation shear on the mode frequency and growth rate by solving eqns. (21) and (13) and substituting in eqn. (15). We begin with some preliminary general discussion. Because of the large exponential factor on the right hand side of eqn. (21), its solution at small $\hat{\Omega}_q$ is given by $s = p+1/2$, leading to the result

$$\frac{(\gamma - i\omega)}{\omega_0} = \left[\frac{\gamma_0}{\omega_0} - i - \left(\frac{\Lambda^2 \hat{\Omega}_q}{2} \right)^2 + \hat{\epsilon} - \frac{(2\hat{\epsilon})^{1/2} (p+1/2)}{\Lambda^2} \right] \quad (23)$$

One expects this behaviour to change when the left-hand side of eqn. (21) competes with the right-hand side, namely when $\hat{\Omega}_q = \hat{\Omega}_q^{\text{crit}} \sim \hat{\epsilon}_0^{1/2} / \Lambda_0^2$. Eventually, at large $\hat{\Omega}_q$ it is clear from eqns. (16) and (19) that $|\sigma| \gg 1$ so that one can expand the integral in this limit. As a consequence we find:

$$\frac{(\gamma - i\omega)}{\omega_0} = \left[\frac{\gamma_0}{\omega_0} + \frac{\hat{\epsilon}^2}{2(\Lambda^2 \hat{\Omega}_q)^2} - \frac{\ell^2}{\Lambda^4} \right] - i - i\ell \hat{\Omega}_q \quad (24)$$

Thus ω and γ asymptote to ω_0 and $\omega_0 + \ell\Omega_q$, respectively, as $\hat{\Omega}_q \rightarrow \infty$ (provided $\ell \ll |\Lambda^2|$), i.e. the ‘cylindrical’ result’ corresponding to the Doppler shift at the ℓ^{th} surface. The form (19) can be used to continue the asymptotic result (24) down to near the point where either: (i) The eigenvalue links to those for lower values of the harmonic p , when the turning points are close together, as given by eqn. (21); (ii) The corresponding anti-Stokes lines intersect with the points $k = 0$ and $k = 2p$ and the passing mode is lost, relevant to higher values of p , in which case one must use eqn. (22); or (iii) The eigenvalue links to intermediate harmonics when one uses eqn. (20). For the special, but interesting, case where $\alpha = \pi/4$ (this corresponds to a radial variation in the lowest order ℓ only) the left-hand side of eqn. (19) is bounded for all $\hat{\Omega}_q$: this means that the conventional ballooning modes can only be displaced from $s = (p+1/2)$ by exponentially small amounts; the passing modes however can respond with s (or $\hat{\sigma}$) changing significantly.

We turn to numerical solutions of the eigenvalue equations. For case (i) above the analytic forms (19) and (21) overlap in a common region of validity, where

$$1 \ll |\sigma| \ll (2\hat{\epsilon})^{1/2} \Lambda^2, \quad (25)$$

and merge with expression (23) for small $\hat{\Omega}_q$. The transition between the two limits requires a numerical solution of eqn. (21) for $s(O_q)$, obtained by using the complex zero-finding code ZERINT [19]. Similarly, for case (ii), forms (19) and (22) overlap in a region

$$1 \ll |\hat{\sigma}| \ll (2\hat{\epsilon})^{1/2} \Lambda^2 \quad (26)$$

There are several parameters to consider for numerical solution: $\hat{\Omega}_q$, which we scan from zero to large values; ω_0^2 which should take large values (computational difficulties limit our calculations to $\omega_0^2 = 20$); the toroidicity parameter $\hat{\epsilon}$ (an interesting range is, say, $1/2 = \hat{\epsilon}_0 = 2$); and the phase angles a ($0 = a = p/4$) and d ($-p/2 = d = 0$) (ω_0 appearing in eqn. (15) can be inserted at the end and does not affect the solution for s). It is interesting to note that one could eliminate one of the parameters involved in determining the intermediate quantity s . This can be done by calculating $\hat{\Omega}_q / \hat{\Omega}_q^{\text{crit}}$ as a function of just $\Lambda_0^2 \sqrt{2\hat{\epsilon}_0}$, α and d . To limit the parameter space investigated we take $\hat{\epsilon}_0 = 2$, which emphasizes toroidal effects, and generally choose $\omega_0^2 = 15$, although some aspects of varying this parameter are explored. Some electron drift wave models suggest $d \sim -p/2$

[6]: we consider this choice, but also a less ‘prejudiced’ choice, $d = -p/4$. For the phase angle a we consider the choices: $a = 0$, corresponding to the profile variation being entirely due to a variation in the growth rate; $\alpha = p/4$, corresponding to it being due to variation in the real frequency; and an intermediate choice in between, $\alpha = p/8$. We refer to the choice $\gamma_0^2 = 15$, $\hat{\epsilon}_0 = 2$, $a = p/8$, $d = -p/4$ and $\gamma_0 = 1$ as the ‘standard case’.

There are three key points to determine: (i) how the conventional ballooning modes, corresponding to roots specified by the integer p in eqn. (23), at least for the lower harmonics, link to the passing modes labelled by the integer ℓ in eqn. (24); i.e., which p and ℓ correspond to each other; (ii) how and at what value of $\hat{\Omega}_q$ the transition from localised to passing modes occurs: and (iii) what are the asymptotic values of γ at large $\hat{\Omega}_q$ - actually, once one has clarified (i), this follows from eqn. (24).

We have carried out some ‘scoping’ studies concerning issue (i) as a function of a for the case of $d = -p/2$, $\hat{\epsilon}_0 = 1/2$ and $\gamma_0^2 = 5$. We find that for small values of a , $p = 0$ links to $\ell = -2$ as $\hat{\Omega}_q$ increases; $p = 1$ and 2 coalesce along the positive real s -axis and then move apart into the complex plane with $p = 1$ linking to $\ell = -3$ and $p = 3$ to $\ell = -1$; $p = 4$ we find links to $\ell = 0$ as $\hat{\Omega}_q$ increases. (For such a modest value of γ_0^2 very few values of p correspond to close turning points, or even trapped orbits; it is more correct to employ eqn. (20) or (22) in this situation – we return to this later.) A pattern can be detected when one examines the movement of the solutions for s in the complex plane as $\hat{\Omega}_q$ increases. The solutions for s for different values for ℓ form a ‘fan’ with negative real parts and with the imaginary parts increasing in the positive direction as ℓ becomes more negative. As a increases the topology of the root movements changes at critical values of a : at $a = 0.19$, $\ell = -2$ and -3 interchange the values of p they link to; at $a = 0.4$ $\ell = -3$ and -4 interchange; at $a = 0.5$, $\ell = -2$ and -1 interchange again. At the same time, with increasing a one finds the lower p values respond less and less to $\hat{\Omega}_q$, whereas the higher p (which tend to be lower ℓ) respond more strongly. (Recall these values, $p \sim \left| (2\hat{\epsilon})^{1/2} \Lambda^2 \right|$ and $\ell \sim 0$, correspond to barely trapped or just passing orbits.) Similar interchanges occur as γ_0^2 increases from 5 to 6 with $a = p/8$: at $\gamma_0^2 = 5.4$, $p = 1$ switches from $\ell = -2$ to $\ell = -4$, whereas at $\gamma_0^2 = 5.5$, $p = 2$ switches from $\ell = -1$ to $\ell = -2$. The pattern also changes with d ; for $d = 0$, $p = 0$ and $p = 1$ exchange ℓ values (i.e. between $\ell = -1$ and $\ell = 0$) at $a = 0.23$; at $a = 0.5$, $p = 0$ changes from $\ell = -1$ to $\ell = -2$, while $p = 1$ changes from $\ell = 0$ to $\ell = -1$.

Clearly the situation is complex in detail but one can draw some general conclusions. Calculations with larger $\gamma_0^2 = 10, 15, 20$ show that the tendency is for the lowest p to be associated with high values of ℓ , whereas $\ell = 0$ appears to be associated with closed orbits ‘sitting’ near the top of the potential well formed by $Q(k)$. As a increases, reaching $-p/2$, the response to $\hat{\Omega}_q$ becomes less for low p modes, while the higher values of p are more sensitive.

We have calculated the response of γ and ω to $\hat{\Omega}_q$ for the standard case. Figure 1 shows the evolution of γ/γ_0 for the root with $p = 0$ as $\hat{\Omega}_q$ increases, illustrating the sharp transition at $\hat{\Omega}_q = \hat{\Omega}_q^{\text{crit}}$. The $\hat{\Omega}_q \rightarrow 0$ limit coincides with the result (23). For large $\hat{\Omega}_q$ we recover the limit (24), but for the choice $\ell = -18$. The large value of $|\ell|$ implies it is much more stable than the $\ell = 0$ solution. The $\ell = 0$ solution is found to correspond to the high harmonic $p = 16$. Figure 2 shows the variation in its growth rate: the sharp kink is real (as can be clearly seen when viewed in the complex s -plane), but the asymptotic matching method connecting eqns. (19) and (21) is breaking down because the inequality (25) is not well satisfied for such large values of s .

This behaviour contrasts with results for the other extreme, but simple, case $a = d = 0$ [10]. As shown in Fig. 3, we find $p = 0$ then links to $\ell = 0$ and $\gamma/\gamma_0 \rightarrow 1$ as $\hat{\Omega}_q \rightarrow \infty$. The roots $p = 1$ and $p = 2$ coalesce, moving off into the complex plane and generating a pair of finite frequency modes with $\omega = \omega_0 \pm \Omega_q$, corresponding to $\ell = \pm 1$, as shown in Fig. 4. Their growth rates also converge to $\gamma/\gamma_0 \rightarrow 1$, as shown in Fig. 5 for $p = 1$. These results are in accordance with the results of Ref. 10 and, also, the ideal MHD ballooning calculations of Ref. 13 to which this problem is isomorphic (at least in the absence of stable values of k , when issues connected with the continuum arise).

The case $\alpha = \pi/4$ and $d = -\pi/2$ has also been examined numerically using eqns. (21). Here one does indeed find that the roots for different p do not respond to $\hat{\Omega}_q$ at all; only when these roots correspond to barely trapped or passing modes sitting at, or beyond, the top of the potential well is there any response. This particular situation has been addressed by solving eqn. (22) for the new eigenvalue $\hat{\sigma}$. Figure 6 shows the dependence of ω on $\hat{\Omega}_q$ for the first few ‘lowest energy’ passing modes: one sees they oscillate, coalescing and separating again. Indeed they form an almost perfect lattice of crossing roots, although there is a slow change in the limits of the oscillations as $\hat{\Omega}_q$ increases. However this picture is not robust to changes in α : even for $\alpha = 15p/32$ the trajectories of the passing modes tend to move to large real $\hat{\sigma}$ as $\hat{\Omega}_q$ increases. It is not possible to follow roots to the far left where $s \sim O(1)$ because the approximations underlying eqn. (22) fail – rather one needs to use eqn. (20).

5. Conclusions

We have developed an analytic dispersion relation that can be used to examine the impact of rotation shear on drift waves, using a generic model for the latter. This model describes cases in which the radial variation of the local eigenvalue from conventional ballooning theory, $\omega(x, k)$, is controlled by that of the growth rate, to where it is the real frequency variation that dominates: this range of cases is parameterised by a phase angle

α . The other key parameters are the normalised rotation shear, $\hat{\Omega}_q$, the mode number, n , encapsulated in the large parameter Λ_0 and a measure of toroidal coupling, $\hat{\epsilon}$, that is characterised by its amplitude, $\hat{\epsilon}_0$, and phase angle, d . The dependence of $Q(x, k)$ on the ballooning angle k is taken to be sinusoidal but a generalisation to other harmonic variation would be straight forward (since it is controlled by the behaviour of $Q(k)$ near $k = 0$ for eqn. (21) - or p for eqn. (22) - and one need only renormalize $\hat{\epsilon}$ to describe more general situations).

General features of the solution of the dispersion relation are evident analytically. There is normally a continuous evolution of the mode and its complex frequency from the conventional ballooning mode at zero flow shear to a ‘passing’ mode at high flow shear. The latter mode is essentially cylindrical in its nature, toroidal effects being averaged out by flow shear: consequently it is more stable. The transition becomes sharper as Λ_0 (i.e. n) increases, defining a critical value: critical value: $\hat{\Omega}_q^{\text{crit}} \sim \sqrt{2\hat{\epsilon}}/\Lambda_0^2 \sim 1/n$. The degree of stabilisation of a particular harmonic, p , of the conventional mode depends on which harmonic, ℓ , of the passing modes it links to, the higher harmonics of the latter being more stable. As numerical solutions show, this is a complex question depending on the parameters of the model, e.g. the phase angle α .

Specific numerical results have been obtained for three special cases. One is where the radial variation is due entirely to the growth rate ($\alpha = 0$) and the toroidal coupling is in phase with the lowest order frequency, $d = -\pi/2$ (the last condition is typical of drift waves). This shows that the most unstable ($p = 0$) harmonic of the conventional ballooning mode becomes a more stable passing mode ($\ell = 0$ - i.e. with zero real frequency shift but the most unstable passing mode) as $\hat{\Omega}_q$ increases. The second and third first harmonics first coalesce and then acquire real frequencies corresponding to $\ell = \pm 1$ as they evolve to the more stable passing modes. The second limiting case is when the radial variation is in the real frequency, $\alpha = p/4$, but $d = -\pi/2$ still. In this case the conventional ballooning modes are essentially untouched by $\hat{\Omega}_q$ but the real frequency of the passing modes at zero $\hat{\Omega}_q$ evolves so as to coalesce with neighbouring ones before returning in a cyclic manner. However this behaviour is not robust to a small change in α : the real parts then evolve without bound. Finally we considered an intermediate, more general, case: $\alpha = p/8$, $d = -p/4$. In this case the lowest harmonic conventional modes link to passing modes with high values of ℓ (and hence are the more stable), whereas a higher harmonic links to the most unstable passing mode, $\ell = 0$.

The key outcome of these studies is that rotation shear rapidly alters the results of conventional ballooning theory, leading to less unstable ‘passing’ modes. Whatever the one-to-one correspondence between conventional and passing modes, the most unstable passing one corresponds to the average of the conventional growth rate over k , thus resembling more the ‘cylindrical’ result corresponding to a mode centred on a single resonant surface. There may, of course, remain some ‘toroidal’ effects arising from sidebands that appear in the calculation of γ_0 .

Of course there are many parameter combinations with complex patterns for the links between the mode numbers p and ℓ but it is interesting to note that we can eliminate one of the parameters involved in determining the intermediate quantity s . This we can do by calculating $\hat{\Omega}_q / \hat{\Omega}_q^{\text{crit}}$ as a function of $\Lambda_0^2 \sqrt{2\hat{\epsilon}_0}$, α and d .

In summary we have provided a technique for evaluating the effect of rotation shear on the stability of a generic drift mode, deducing some general trends and evaluating some limiting cases numerically. In future this technique could be applied to specific examples of drift waves.

Acknowledgments

This work was jointly funded by the United Kingdom Engineering and Physical Sciences Research Council and by EURATOM. The views and opinions expressed herein do not necessarily reflect those of the European Commission.

References

- [1] Connor, J. W., Hastie, R. J. and Taylor, J. B., Proc. R. Soc. London A **365** (1979) 1.
- [2] Glasser, A. H., in Proceedings of the Finite-Beta Workshop (Varenna, Italy, September 1977) (ed. by Coppi, B. and Sadowski, W.), p. 55. National Technical Information Service, Springfield, Virginia, 1979.
- [3] Lee, Y. C. and Van Dam, J. W., in Proceedings of the Finite-Beta Workshop (Varenna, Italy, September 1977) (ed. by Coppi, B. and Sadowski, W.), p. 93. National Technical Information Service, Springfield, Virginia, 1979.
- [4] Pegoraro, F. and Schep, T. J., Phys. Fluids **8** (1981) 315.
- [5] Connor, J. W., Taylor, J. B. and Wilson, H. R., Phys. Rev. Lett. **70** (1993) 1803.
- [6] Taylor, J. B., Connor, J. W. and Wilson, H. R., Plasma Phys. Control. Fusion **35** (1993) 1063.
- [7] Connor, J. W., Hastie, R. J. and Taylor, J. B., Plasma Phys. Control. Fusion **46** (2004) B1.
- [8] Dewar, R. L., in *Theory of Fusion Plasmas*, edited by Bondeson, A., Sindoni, E. and Troyon, F. (Societa Italiana di Fisica, Bologna, 1987), p. 107.
- [9] Zhang, Y. Z. and Mahajan, S. M., Phys. Lett. **157A** (1991) 133.
- [10] Dewar, R. L., Plasma Phys. Control. Fusion **39** (1997) 453.
- [11] Taylor, J. B. and Wilson, H. R., Plasma Phys. Control. Fusion **38** (1996) 1999.
- [12] Waelbroeck, F. L. and Liu Chen, Phys. Fluids B **3** (1991) 601.
- [13] Connor, J. W., Hastie, R. J. and Martin, T. J., in *Theory of Fusion Plasmas*, edited by Connor, J. W., Sauter, O. and Sindoni, E. (Societa Italiana di Fisica, Bologna, 2004), p. 457.
- [14] Erdélyi, A. et al., in *Higher Transcendental Functions* (McGraw-Hill, New York, 1955), Vol. **III**, p. 91.
- [15] Langer, R. E., Trans. American Math. Society, **36**, 637 (1934).
- [16] Heading, J., *An Introduction to Phase-Integral Methods*, (Methuen, London, 1962).
- [17] Romanelli, F. and Zonca, F., Phys. Fluids B **5** (1993) 4081.

- [18] Davies, P. J., in *Handbook of Mathematical Functions*, eds. M. Abramowitz and I. A. Stegun (Dover, New York, 1965), Sec. **6**, p. 253.
- [19] Martin, T. J., private communication.
- [20] Antosiewicz, H. A., in *Handbook of Mathematical Functions*, eds. M. Abramowitz and I. A. Stegun (Dover, New York, 1965), Sec. **10.4**, p. 446.
- [21] Miller, J. C. P., in *Handbook of Mathematical Functions*, eds. M. Abramowitz and I. A. Stegun (Dover, New York, 1965), Sec. **19**, p. 685.
- [22] Whittaker, E. A. and Watson, G. N., in *A Course of Modern Analysis* (Cambridge University Press, Cambridge, 1927), Sec.**16.5**, p. 347.

Appendix A – Derivation of $\xi(2\pi)$ for general turning points: Equation (20)

For $|\Lambda^2| \gg 1$ we can seek WKB solutions of eqn.(12).

$$\xi = \sum_{\pm} \frac{C_{\pm}}{Q^{1/4}} \exp(\pm i \int^k Q^{1/2} dk) \quad (\text{A.1})$$

The turning points, where $Q(k)=0$, are given by

$$\sin^2\left(\frac{k_0}{2}\right) = \frac{\sigma}{(2\hat{\epsilon})^{1/2} \Lambda^2} \quad (\text{A.2})$$

Near $k = k_0$ we introduce

$$z = \left[\frac{\Lambda^4 (2\hat{\epsilon}) \sin k_0}{2} \right]^{1/3} (k - k_0) \quad (\text{A.3})$$

so that

$$\int_{k_0}^k Q^{1/2} dk = -\frac{2}{3} (-z)^{3/2} \quad (\text{A.4a})$$

$$Q^{1/4} = Cz^{1/4}, \quad C \text{ a constant} \quad (\text{A.4b})$$

We suppose the anti-Stokes lines [16] emanating from k_0 are such that the solution oscillates along the line $(-k_0, k_0)$

Between the turning points $\pm k_0$ we can write the even WKB solution as

$$\xi_{\text{WKB}}(k) = \frac{1}{Q^{1/4}} \cos\left(\int_0^k Q^{1/2} dk\right) \quad (\text{A.5})$$

Using the form (A.3)

$$\int_0^{k_0} Q^{1/2} dk = I_0 - \frac{2}{3}(-z)^{3/2} \quad (\text{A.6})$$

near $k = k_0$, where

$$I_0 = \int_0^{k_0} Q^{1/2} dk \quad (\text{A.7})$$

To continue this past the turning points we examine eqn.(12) in their vicinity. It takes the form of Airy's equation [20]

$$\left(\frac{d^2}{dz^2} - z\right)\xi = 0 \quad (\text{A.8})$$

with solutions $A_i(z), B_i(z)$ [20]. These have the asymptotic forms

$$A_1(z) \sim \frac{1}{\sqrt{\pi z}^{1/4}} \sin(\zeta + \pi/4) \quad |\text{Arg } z| < 2\pi/3$$

$$B_1(z) \sim \frac{1}{\sqrt{\pi z}^{1/4}} \cos(\zeta + \pi/4) \quad |\text{Arg } z| < 2\pi/3 \quad (\text{A.9})$$

$$A_1(-z) \sim \frac{1}{2\sqrt{\pi z}^{1/4}} e^{-\zeta} \quad |\text{Arg } z| < \pi$$

$$B_1(-z) \sim \frac{1}{\sqrt{\pi z}^{1/4}} e^{\zeta} \quad |\text{Arg } z| < \pi/3 \quad (\text{A.10})$$

where $\zeta = \frac{2}{3}z^{3/2}$. The form (A.4) can be written as

$$\begin{aligned} \xi_{\text{WKB}} = & \frac{1}{Cz^{1/4}} \cos\left(I_0 + \frac{\pi}{4}\right) \cos\left[\frac{2}{3}(-z)^{3/2} + \frac{\pi}{4}\right] \\ & + \sin\left(I_0 + \frac{\pi}{4}\right) \sin\left[\frac{2}{3}(-z)^{3/2} + \frac{\pi}{4}\right] \end{aligned} \quad (\text{A.11})$$

which matches to

$$\xi = \frac{\sqrt{\pi}}{C} \left[B_1(-z) \cos\left(I_0 + \frac{\pi}{4}\right) + A_1(-z) \sin\left(I_0 + \frac{\pi}{4}\right) \right] \quad (\text{A.12})$$

Using the asymptotic forms (A.9) and (A.10) and the result (A.3) we can continue ξ through to k_0 to obtain

$$\xi_{\text{WKB}} = \frac{1}{(-Q)^{1/4}} \left\{ \cos\left(I_0 + \frac{\pi}{4}\right) \exp\left[\int_{k_0}^k (-Q)^{1/2} dk\right] + \frac{1}{2} \sin\left(I_0 + \frac{\pi}{4}\right) \exp\left[-\int_{k_0}^k (-Q)^{1/2} dk\right] \right\} \quad (\text{A.13})$$

Near the next turning point of $k = 2\pi - k_0$ we can write

$$\int_{k_0}^k (-Q)^{1/2} dk = I_1 - \zeta'; \quad I_1 = \int_{k_0}^{2\pi - k_0} (-Q)^{1/2} dk \quad (\text{A.14})$$

where

$$\zeta' = \frac{2}{3}(z')^{3/2}, \quad z' = 2\pi - k_0 - k$$

Again using the asymptotic forms (A.9) and (A.10) to continue ξ through $2\pi - k_0$, we obtain

$$\xi_{\text{WKB}}(2p) = \frac{1}{Q^{1/4}} \left\{ 2 \cos\left(I_0 + \frac{\pi}{4}\right) \sin\left(I_2 + \frac{\pi}{4}\right) \exp(I_1) + \frac{1}{2} \sin\left(I_0 + \frac{\pi}{4}\right) \cos\left(I_2 + \frac{\pi}{4}\right) \exp(-I_1) \right\} \quad (\text{A.15})$$

where $I_2 = \int_{2\pi - k_0}^{2\pi} Q^{1/2} dk = I_0$ by symmetry. Then

$$\frac{\xi(2\pi)}{\xi(0)} = \left[\cos(2I_0) \exp(I_1) + \frac{1}{4} \exp(-I_1) \right] \quad (\text{A.16})$$

Appendix B – Derivation of $\xi(2\pi)$ for close turning parts: Equation (21)

To derive eqn.(21) we must solve eqn. (12) for $\xi(k)$ with the boundary condition $d\xi/dk = 0$ at $k = 0$, assuming $|\Lambda^2| \gg 1$. We suppose $0 \leq \alpha \leq \pi/4$ and $-\pi/2 \leq \gamma \leq 0$, which serves to locate the position of the turning points of eqn.(12) in the complex k -plane. Near $k = 0$, eqn.(12) can be written in the form of the Parabolic Cylinder equation (or Weber's equation) [21, 22]:

$$\left\{ \frac{d^2}{dz^2} + \sigma - \frac{z^2}{4} \right\} \xi = 0 \quad (\text{B.1})$$

where $z = \Lambda(2\hat{\epsilon})^{1/4} k$. Thus the real k -axis corresponds to

$$-\frac{\pi}{4} \leq \text{Arg } z \leq \frac{\pi}{4} \quad (\text{B.2})$$

The even solution of eqn. (B.1) is

$$\xi(z) = D_{\sigma-1/2}(z) + D_{\sigma-1/2}(-z) \quad (\text{B.3})$$

where $D_{\sigma-1/2}$ is the Parabolic Cylinder Function [21, 22],

$$\xi(0) = 2D_{\sigma-1/2}(0) \quad (\text{B.4})$$

Away from $k = 0$, we must match $\xi(z)$ at large $|z|$ to the WKB solution [16] of eqn. (12):

$$\xi_{\text{WKB}}(k) = \frac{C_+}{Q^{1/4}} \exp(i \int_{k_0}^k Q^{1/2} dk) + \frac{C_-}{Q^{1/4}} \exp(-i \int_{k_0}^k Q^{1/2} dk) \quad (\text{B.5})$$

Here $k_0 = 2\sigma^{1/2}(2\hat{\epsilon})^{-1/4} \Lambda^{-1}$ is the turning point $z = 2\sigma^{1/2}$ of eqn. (B.1) Taking account of the condition (B.2) we need the following asymptotic forms of $D_{\sigma-1/2}(z)$ [21, 22]:

$$D_{\sigma-1/2}(z) \sim z^{\sigma-1/2} e^{-z^2/4}, \quad -3\pi/4 < \text{Arg } z < 3\pi/4 \quad (\text{B.6})$$

$$D_{\sigma-1/2}(z) \sim z^{\sigma-1/2} e^{-z^2/4} - \frac{\sqrt{2\pi}}{\Gamma(1/2-\sigma)} e^{i\pi(\sigma-1/2)} z^{-(\sigma+1/2)} e^{z^2/4}, \quad \pi/4 < \text{Arg } z < 5\pi/4 \quad (\text{B.7})$$

Using the limit (B.6) for $D_{\sigma-1/2}(z)$ and (B.7) for $D_{\sigma-1/2}(-z)$ in eqn. (B.3), we have

$$\xi(z) \sim z^{\sigma-1/2} e^{-z^2/4} (1 + e^{i\pi(\sigma-1/2)}) + \frac{\sqrt{2\pi}}{\Gamma(1/2-\sigma)} z^{-(\sigma-1/2)} e^{z^2/4} \quad (\text{B.8})$$

This must be matched to the $|k_0| \ll k \ll 1$ limit of eqn. (B.5) where

$$\begin{aligned} i \int_{k_0}^k Q^{1/2} dk &= 2\sigma \int_1^{z/(2\sigma^{1/2})} (u^2 - 1)^{1/2} du \\ &= \frac{z^2}{4} - \frac{\sigma}{2} - \sigma \ln(z/\sigma^{1/2}), \quad |z| \gg |2\sigma^{1/2}| \end{aligned} \quad (\text{B.9})$$

and $Q^{1/4} \simeq Cz^{1/2}$ where C is a constant. Then eqn. (B.5) takes the form

$$\begin{aligned} \xi_{\text{WKB}}(z) &\sim \frac{C_+ \sigma^{(\sigma/2)}}{Cz^{(1/2+\sigma)}} \exp\left(\frac{z^2}{4} - \frac{\sigma}{2}\right) \\ &\quad + \frac{C_- \sigma^{-(\sigma/2)}}{Cz^{(1/2-\sigma)}} \exp\left(-\frac{z^2}{4} + \frac{\sigma}{2}\right) \end{aligned} \quad (\text{B.10})$$

Clearly eqns. (B.8) and (B.10) can be matched and we can identify C_{\pm} . However the term proportional to C_+ is exponentially growing and we can ignore the exponentially decaying term proportional to C_- . Thus

$$\frac{C_+}{C} e^{-\sigma/2} \sigma^{\sigma/2} = \frac{\sqrt{2\pi}}{\Gamma(1/2-\sigma)} \quad (\text{B.11})$$

We can now propagate this growing exponential term to near the next turning point at $k_1 = 2\pi - k_0$ using the WKB form. Approaching k_1 , we can write

$$i \int_{k_0}^k Q^{1/2} dk = \hat{I}_1 - 2\sigma \int_1^{z'/(2\sigma^{1/2})} (u^2 - 1)^{1/2} du \quad (\text{B.12})$$

where

$$\hat{I}_1 = \int_{k_0}^{k_1} (-Q)^{1/2} dk = \Lambda^2 (2\hat{\epsilon})^{1/2} \int_{k_0}^{2\pi - k_0} dk \left[\sin^2\left(\frac{k}{2}\right) - \frac{\sigma}{(2\hat{\epsilon})^{1/2} \Lambda^2} \right]^{1/2} \quad (\text{B.13})$$

and $z' = \Lambda(2\hat{\epsilon})^{1/4}(2\pi - k)$. Then

$$\xi_{\text{WKB}} \sim \frac{C_+ \sigma^{-(\sigma/2)}}{C Z^{(\frac{1}{2}-\sigma)}} \exp\left(\hat{I}_1 + \frac{\sigma}{2} - \frac{z'^2}{4}\right) \quad (\text{B.14})$$

Near $k \sim 2\pi$, eqn. (12) again reduces to the Parabolic Cylinder equation (B.1), but with $z \rightarrow z'$. The WKB form (B.14) clearly matches to the asymptotic form (B.6) for $|z'| \gg 1$. Thus, with the aid of result (B.11)

$$\xi(2\pi) = \frac{\sqrt{2\pi} \sigma^{-\sigma}}{\Gamma(\frac{1}{2} - \sigma)} \exp(\hat{I}_1 + \sigma) D_{\sigma - 1/2}(0) \quad (\text{B.15})$$

It remains to evaluate the integral \hat{I}_1 in eqn. (B.13):

$$\hat{I}_1 = 4\Lambda^2 (2\hat{\epsilon})^{1/2} \int_{k_0/2}^{\pi/2} du (\sin^2 u - \delta^2)^{1/2} \quad (\text{B.16})$$

$$\delta^2 = \frac{\sigma}{(2\hat{\epsilon})^{1/2} \Lambda^2}, \quad |\delta| \ll 1$$

We introduce $\eta: |\delta| \ll \eta \ll \pi/2$, so that

$$\frac{\hat{I}_1}{4\Lambda^2 (2\hat{\epsilon})^{1/2}} = \bar{I}_1 + \bar{I}_2 \quad (\text{B.17})$$

where

$$\bar{I}_1 = \int_{\delta}^{\eta} (u^2 - \delta^2)^{1/2} du, \quad \bar{I}_2 = \int_{\eta}^{\pi/2} \sin u \left(1 - \frac{\delta^2}{2\sin^2 u}\right) du \quad (\text{B.18})$$

We find

$$\bar{I}_1 = \frac{\eta^2}{2} - \frac{\delta^2}{4} - \frac{\delta^2}{2} \ln\left(\frac{2\eta}{\delta}\right), \quad \eta \gg |\delta| \quad (\text{B.19})$$

$$\begin{aligned} \bar{I}_2 &= \cos \eta + \frac{\delta^2}{4} \ln\left(\frac{1 - \cos \eta}{1 + \cos \eta}\right) \\ &\approx 1 - \frac{\eta^2}{2} + \frac{\delta^2}{4} \ln\left(\frac{\eta^2}{4}\right), \quad \eta \gg |\delta| \end{aligned} \quad (\text{B.20})$$

Thus

$$\bar{I}_1 + \bar{I}_2 = 1 - \frac{\delta^2}{4} - \frac{\delta^2}{2} \ln\left(\frac{4}{\delta}\right) \quad (\text{B.21})$$

so that

$$\hat{I}_1 = 4\Lambda^2 (2\hat{\epsilon})^{1/2} - \sigma - \sigma \ln\left[\frac{16(2\hat{\epsilon})^{1/2} \Lambda^2}{\sigma}\right] \quad (\text{B.22})$$

Combining results (B.4), (B.15) and (B.22), we finally have

$$\frac{\xi(2\pi)}{\xi(0)} = \frac{\sqrt{2\pi}}{2\Gamma(1/2 - \sigma)} (16(2\hat{\epsilon})^{1/2} \Lambda^2)^{-\sigma} \exp\left[4\Lambda^2 (2\hat{\epsilon})^{1/2}\right] \quad (\text{B.23})$$

Using Stirling's formula for the asymptotic forms of the Gamma functions at large s [20], one finds the result (B.23) smoothly matches to eqn. (18).

There is a ready generalisation of eqn (B.23) for more complex poloidal variations. Thus if, for a periodic function $f(k)$,

$$\hat{\epsilon} \cos k \rightarrow f(k) \approx f_0 - f_1 k^2 / 2 \quad (\text{B.24})$$

at small k , then we replace $\hat{\epsilon}$ by f_1 .

Appendix C: – Derivation of $\xi(2\pi)$ for two turning points near $k = p$: Equation (22)

If $Q(k)$ has its zeros near $k = \pi$ it is again possible to obtain an analytic dispersion relation; indeed this is necessary to reveal the behaviour of σ in this region of parameters. We introduce $k = \pi \pm \kappa$, where the signs corresponds to $k \lesseqgtr \pi$. Then one can simplify eqn. (14) to yield

$$\left\{ \frac{1}{\epsilon^2} \frac{d^2}{dk^2} + 2\hat{\epsilon} \left(\frac{\hat{\sigma}}{\sqrt{2\hat{\epsilon}} \epsilon^2} + \frac{\kappa^2}{4} \right) \right\} \xi = 0 \quad (C.1)$$

where

$$\hat{\sigma} = \sigma - \sqrt{2\hat{\epsilon}} \epsilon^2 \quad (C.2)$$

Introducing

$$t = \pm e^{i\pi/4} \epsilon \sqrt{2\hat{\epsilon}} \kappa \quad (C.3)$$

eqn.(C.1) takes the form

$$\left\{ \frac{d^2}{dt^2} - i\hat{\sigma} - \frac{t^2}{4} \right\} \xi = 0 \quad (C.4)$$

with Parabolic Cylinder Functions, $D_{-i\hat{\sigma}-1/2}(\pm t)$. Then solutions must be matched to the WKB solution of eqn. (12) satisfying $(d\xi/dk)_0 = 0$:

$$\xi_{\text{WKB}} = \frac{1}{Q^{1/4}} \cos\left(\int_0^k Q^{1/2} dk\right) \quad (C.5)$$

To determine the behaviour of ξ near $k = \pi$ we write

$$i \int_0^k Q^{1/2} dk = i \int_0^\pi Q^{1/2} dk - i \int_0^k Q^{1/2}(\kappa) dk, \quad k < \pi \quad (C.6)$$

Using

$$Q = \sqrt{2\hat{\epsilon}} \epsilon^2 \left(\frac{\hat{\sigma}}{\sqrt{2\hat{\epsilon}} \epsilon^2} + \frac{\kappa^2}{4} \right) \quad (C.7)$$

and with the substitution

$$k = 2\left(\frac{\hat{\sigma}}{\sqrt{2\hat{\epsilon}} \epsilon^2}\right)^{1/2} u,$$

$$i \int_0^k Q^{1/2} dk = i \tilde{I}_0 - 2i\hat{\sigma} \int_0^u (1+u^2) du \quad (C.8)$$

where

$$\tilde{I}_0 = \int_0^\pi Q^{1/2} dk \quad (C.9)$$

The integral over u is given by

$$I = \int_0^u (1+u)^{1/2} du = \frac{1}{2} \left[u\sqrt{1+u^2} + \ln(u + \sqrt{1+u^2}) \right] \quad (C.10)$$

and, since we need to match to the WKB solution at large $|u|$, has the asymptotic form

$$I = \frac{1}{2} (u^2 + \frac{1}{2} + \ln 2u) \quad (C.11)$$

Here $u = -te^{-i\pi/4} / 2\sqrt{\hat{\sigma}}$ and we use the sign convention of Whittaker and Watson [22] so that $u = e^{3i\pi/4} / 2\sqrt{\hat{\sigma}}$, we obtain

$$i \int_0^k Q^{1/2} dk = i\tilde{I}_0 - \frac{t^2}{4} - i\hat{\sigma} \ln t + \frac{i\hat{\sigma}}{2} \ln \hat{\sigma} - \frac{3\hat{\sigma}\pi}{4} \quad (C.12)$$

Furthermore, for $k < \pi$, $Q^{1/4} \propto (\kappa^2)^{1/4} \propto e^{3i\pi/16} t^{1/2}$. Thus, near $k = \pi$

$$\begin{aligned} \xi_{\text{WKB}} = & \frac{1}{2e^{3i\pi/16}} \frac{1}{(\hat{\sigma})^{i\hat{\sigma}/2}} \left\{ \exp \left[-i\tilde{I}_0 + \frac{i\hat{\sigma}}{2} + \frac{3\hat{\sigma}\pi}{4} - \frac{t^2}{4} \right] t^{-1/2+i\hat{\sigma}} \right. \\ & \left. + (\hat{\sigma})^{i\hat{\sigma}/2} \exp \left[i\tilde{I}_0 - \frac{i\hat{\sigma}}{2} - \frac{3\hat{\sigma}\pi}{4} + \frac{t^2}{4} \right] t^{-1/2-i\hat{\sigma}} \right\} \end{aligned} \quad (C.13)$$

For $k = \pi$, $\text{Arg } t = -3p/4 + \alpha/2 + \gamma/4$, where $t^2 = t_0^2 e^{i\alpha}$ and $\hat{\varepsilon} = \hat{\varepsilon}_0 e^{i\gamma}$, with $0 < \alpha < \pi/4$ and $\pi/2 < \gamma < 0$, so that $-7p/8 < \text{Arg } t < -5p/8$. On the other hand, $p/8 < \text{Arg}(-t) < 3p/8$. The asymptotic forms of $D_{-1/2-i\hat{\sigma}}(u)$ in relevant regions are

$$\begin{aligned}
D_{-\frac{1}{2}-i\hat{\sigma}}(u) &\sim u^{-\frac{1}{2}-i\hat{\sigma}} e^{-u^{\frac{1}{4}}}, & |\text{Arg } u| < 3\pi/4 \\
D_{-\frac{1}{2}-i\hat{\sigma}}(u) &\sim u^{-\frac{1}{2}-i\hat{\sigma}} e^{-u^{\frac{1}{4}}} - \frac{\sqrt{2\pi}}{\Gamma(\frac{1}{2}+i\hat{\sigma})} e^{i\pi(\frac{1}{2}+i\hat{\sigma})} u^{-(\frac{1}{2}-i\hat{\sigma})} e^{u^{\frac{1}{4}}}, & -5\pi/4 < \text{Arg } u < -\pi/4
\end{aligned} \tag{C.14}$$

which can be matched to ξ_{WKB} .

Thus

$$\begin{aligned}
t^{-\frac{1}{2}-i\hat{\sigma}} e^{-t^{\frac{1}{4}}} &\rightarrow e^{i\pi(\frac{1}{2}+i\hat{\sigma})} D_{-\frac{1}{2}-i\hat{\sigma}}(-t) \\
t^{-\frac{1}{2}+i\hat{\sigma}} e^{t^{\frac{1}{4}}} &\rightarrow e^{-i\pi(\frac{1}{2}+i\hat{\sigma})} \frac{\Gamma(\frac{1}{2}+i\hat{\sigma})}{\sqrt{2\pi}} \left[e^{i\pi(\frac{1}{2}+i\hat{\sigma})} D_{-\frac{1}{2}-i\hat{\sigma}}(-t) - D_{-\frac{1}{2}-i\hat{\sigma}}(t) \right]
\end{aligned} \tag{C.15}$$

We use these relations to continue ξ through to $k > \pi$, where $p/8 < \text{Arg } t < 3p/8$ and $-7p/8 < \text{Arg}(-t) < 5p/8$. Introducing the asymptotic forms for $D_{-\frac{1}{2}-i\hat{\sigma}}(\pm t)$ in this region we have the correspondences

$$\begin{aligned}
t^{-\frac{1}{2}-i\hat{\sigma}} e^{t^{\frac{1}{4}}} &\rightarrow 2i \frac{\Gamma(\frac{1}{2}+i\hat{\sigma})}{\sqrt{2\pi}} \cosh(\hat{\sigma}\pi) t^{-\frac{1}{2}-i\hat{\sigma}} e^{-t^{\frac{1}{4}}} + t^{-\frac{1}{2}+i\hat{\sigma}} e^{t^{\frac{1}{4}}} \\
t^{-\frac{1}{2}-i\hat{\sigma}} e^{-t^{\frac{1}{4}}} &\rightarrow e^{-2\pi\hat{\sigma}} t^{-\frac{1}{2}-i\hat{\sigma}} e^{-t^{\frac{1}{4}}} + \frac{i\sqrt{2\pi}}{\Gamma(\frac{1}{2}+i\hat{\sigma})} e^{-\pi\hat{\sigma}} t^{-\frac{1}{2}+i\hat{\sigma}} e^{t^{\frac{1}{4}}}
\end{aligned} \tag{C.16}$$

We now match these to a WKB solution for ζ for $k > \pi$, namely

$$\xi_{\text{WKB}} = \frac{1}{Q^{\frac{1}{4}}} \left[A \exp\left(i \int_{\pi}^k Q^{\frac{1}{2}} dk \right) + B \exp\left(-i \int_{\pi}^k Q^{\frac{1}{2}} dk \right) \right] \tag{C.17}$$

We note that, now with $k = \pi + \kappa$ so that $t = e^{i\pi/4} \sqrt{2\hat{\epsilon}} \kappa$

$$i \int_{\pi}^k Q^{\frac{1}{2}} dk \rightarrow \frac{t^2}{4} + i\hat{\sigma} \ln t + \frac{i\hat{\sigma}}{2} - i\hat{\sigma} \ln \hat{\sigma} + \frac{\hat{\sigma}\pi}{4} \tag{C.18}$$

at large $|t|$; we also note that $Q^{\frac{1}{4}} \propto e^{-i\pi/6} t^{\frac{1}{2}}$.

Using this formula we can calculate A and B by matching and compute $\xi(2\pi)/\xi(0)$.

Thus

$$\begin{aligned} \frac{\xi(2\pi)}{\xi(0)} &= \sqrt{\frac{\pi}{2}} \frac{e^{2iI_0 - i\hat{\sigma} - \hat{\sigma}\pi/2}}{\Gamma(1/2 + i\hat{\sigma})} (\hat{\sigma})^{i\hat{\sigma}} \\ &+ \frac{1}{\sqrt{2\pi}} e^{-2iI_0 + i\hat{\sigma} - \hat{\sigma}\pi/2} (\hat{\sigma})^{-i\hat{\sigma}} \cosh(\hat{\sigma}\pi) \Gamma(1/2 + i\hat{\sigma}) \end{aligned} \quad (C.19)$$

where we have used $\int_{\pi}^{2\pi} Q^{1/2} dk = \tilde{I}_0$ by symmetry. It remains to calculate \tilde{I}_0 ; substituting $k = \pi - 2\lambda$

$$\tilde{I}_0 = \frac{2}{\delta^2} \int_0^{\pi/2} (\hat{\sigma}\delta^2 + \sin^2 \lambda)^{1/2} d\lambda; \delta^2 = \frac{1}{\sqrt{2\hat{\epsilon}^2}}, |\delta| \ll 1 \quad (C.20)$$

Introducing $\eta: |\hat{\delta}| < |\eta| < \pi/2$, and separating the integration into regions where simplifications are possible,

$$\tilde{I}_0 = \frac{2}{\delta^2} \left\{ \int_0^{\eta} (\hat{\sigma}\delta^2 + \lambda^2)^{1/2} d\lambda + \int_{\eta}^{\pi/2} \sin \lambda \left(1 + \frac{\hat{\sigma}\delta^2}{2\sin^2 \lambda}\right) d\lambda \right\} \quad (C.21)$$

These two integrals can be readily evaluated to yield

$$2\tilde{I}_0 = 4\sqrt{2\hat{\epsilon}^2} + \hat{\sigma} + \hat{\sigma} \ln \left(\frac{16\sqrt{2b^2}}{\hat{\sigma}} \right) \quad (C.22)$$

Combining eqns. (C.19) and (C.22) we finally obtain

$$\begin{aligned} \frac{\xi(2\pi)}{\xi(0)} &= \sqrt{\frac{\pi}{2}} \frac{\exp\left(4i\sqrt{2\hat{\epsilon}^2} - \frac{\hat{\sigma}\pi}{2}\right)}{\Gamma(1/2 + i\hat{\sigma})} (16\sqrt{2\hat{\epsilon}^2})^{i\hat{\sigma}} \\ &+ \frac{\Gamma(1/2 + i\hat{\sigma})}{\sqrt{2\pi}} \cosh(\hat{\sigma}\pi) \exp\left(-4i\sqrt{2\hat{\epsilon}^2} - \frac{\hat{\sigma}\pi}{2}\right) (16\sqrt{2\hat{\epsilon}^2})^{-i\hat{\sigma}} \end{aligned} \quad (C.23)$$

Using the reflection formula for Gamma Functions this can be written in a more symmetric form:

$$\frac{\xi(2\pi)}{\xi(0)} = \sqrt{\frac{\pi}{2}} \exp\left(-\frac{\hat{\sigma}\pi}{2}\right) \left[\frac{\exp\left(4i\sqrt{2\hat{\epsilon}}\hat{\sigma}^2\right)}{\Gamma(1/2 + i\hat{\sigma})} (16\sqrt{2\hat{\epsilon}}\hat{\sigma}^2)^{i\hat{\sigma}} + \frac{\exp\left(-4i\sqrt{2\hat{\epsilon}}\hat{\sigma}^2\right)}{\Gamma(1/2 - i\hat{\sigma})} (16\sqrt{2\hat{\epsilon}}\hat{\sigma}^2)^{-i\hat{\sigma}} \right] \quad (\text{C.24})$$

Again using Stirling's Formula for the asymptotic forms of the Gamma functions at large s [18], one finds the result (C.23) smoothly matches to eqns. (18) and (20) in appropriate limits.

Figure Captions

Fig. 1: The variation of the normalised growth rate, γ/ω_0 , with increasing flow shear, $\hat{\Omega}_q$, for the lowest, most unstable, conventional ballooning mode harmonic, $p = 0$ for the standard case: $\Lambda_0^2 = 15$, $\hat{\epsilon}_0 = 2$, $\alpha = p/4$, $d = -p/2$, $\gamma_0/\omega_0 = 1$. In this case $p = 0$ evolves into the most unstable passing harmonic $\ell = -18$.

Fig. 2: The variation of the normalised growth rate, γ/ω_0 , with increasing flow shear, $\hat{\Omega}_q$, for the marginally trapped, most stable, conventional ballooning mode harmonic, $p = 16$, for the intermediate case: $\Lambda_0^2 = 15$, $\hat{\epsilon}_0 = 2$, $\alpha = p/8$, $d = -p/4$, $\gamma_0/\omega_0 = 1$. In this case $p = 16$ evolves into the most unstable passing harmonic, $\ell = 0$. However the asymptotic matching method is beginning to break down.

Fig. 3: The variation of the normalised growth rate, γ/ω_0 , with increasing flow shear, $\hat{\Omega}_q$, for the lowest conventional ballooning mode harmonic, $p = 0$, for the case with only a radial profile for the growth rate: $\Lambda_0^2 = 15$, $\hat{\epsilon}_0 = 2$, $\alpha = d = 0$, $\gamma_0/\omega_0 = 1$.

Fig. 4: The variation of normalised frequencies, ω/ω_0 , with $\hat{\Omega}_q$ for the $p = 1$ and 2 harmonics for the case in Fig. 3, showing a coalescence of the two roots and the onset of two real frequencies.

Fig. 5: As for Fig. 3, but for the next two harmonic, $p = 1$.

Fig. 6: The variation of the frequencies of some of the lowest passing harmonics of the conventional ballooning mode as $\hat{\Omega}_q$ increases for the case when there is only a radial variation of the real frequency: $\Lambda_0^2 = 15$, $\hat{\epsilon}_0 = 2$, $\alpha = p/4$, $d = -p/2$, $\gamma_0/\omega_0 = 1$. The full lines are complete calculations, the dashed lines are merely indicative, but do join computed minima and maxima of roots. One sees multiple coalescences.

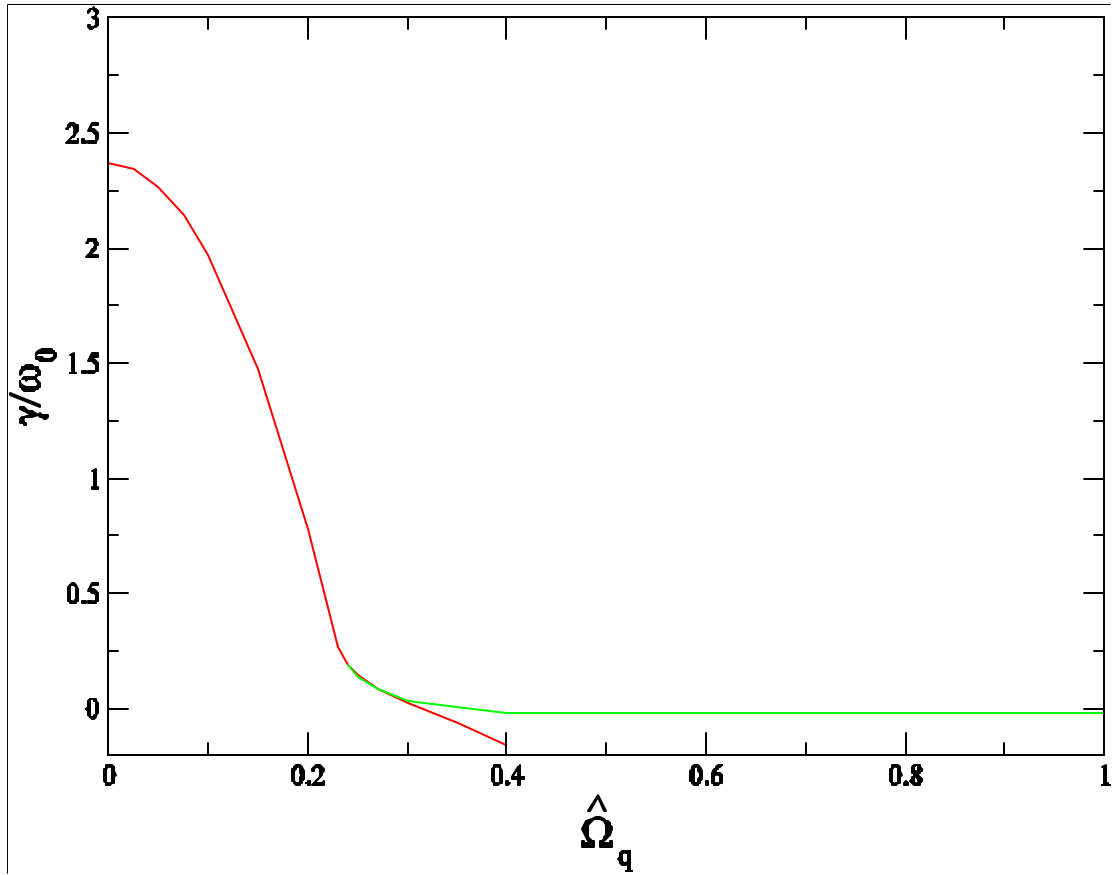


Fig. 1: The variation of the normalised growth rate, γ/ω_0 , with increasing flow shear, $\hat{\Omega}_q$, for the lowest, most unstable, conventional ballooning mode harmonic, $p = 0$, for the standard case: $\Lambda_0^2 = 15$, $\hat{\epsilon}_0 = 2$, $\alpha = p/4 d = -p/2$, $\gamma_0/\omega_0 = 1$. In this case $p = 0$ evolves into the most unstable passing harmonic $\ell = -18$.

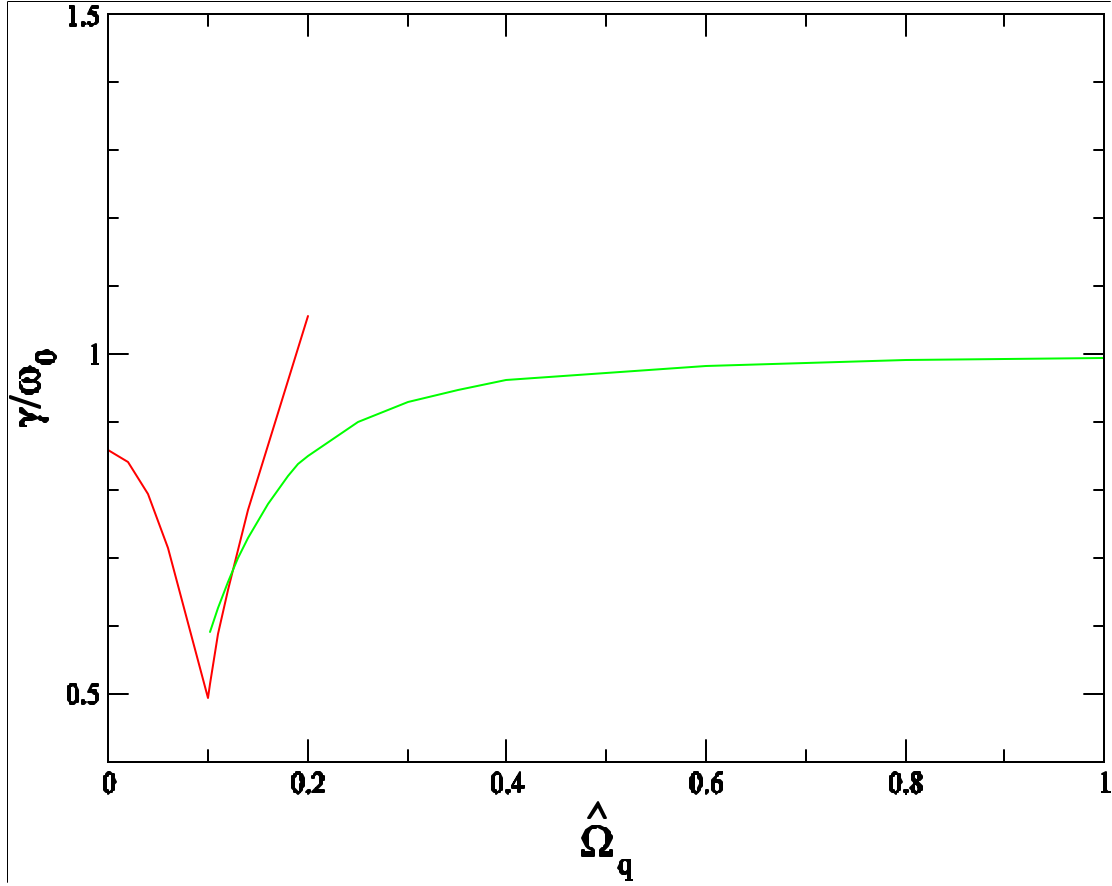


Fig. 2: The variation of the normalised growth rate, γ/ω_0 , with increasing flow shear, $\hat{\Omega}_q$, for the marginally trapped, most stable, conventional ballooning mode harmonic, $p = 16$, for the intermediate case: $\Lambda_0^2 = 15$, $\hat{\epsilon}_0 = 2$, $\alpha = p/8$, $d = -p/4$, $\gamma_0/\omega_0 = 1$. In this case $p = 18$ evolves into the most unstable passing harmonic, $\ell = 0$. However the asymptotic matching method is beginning to break down.

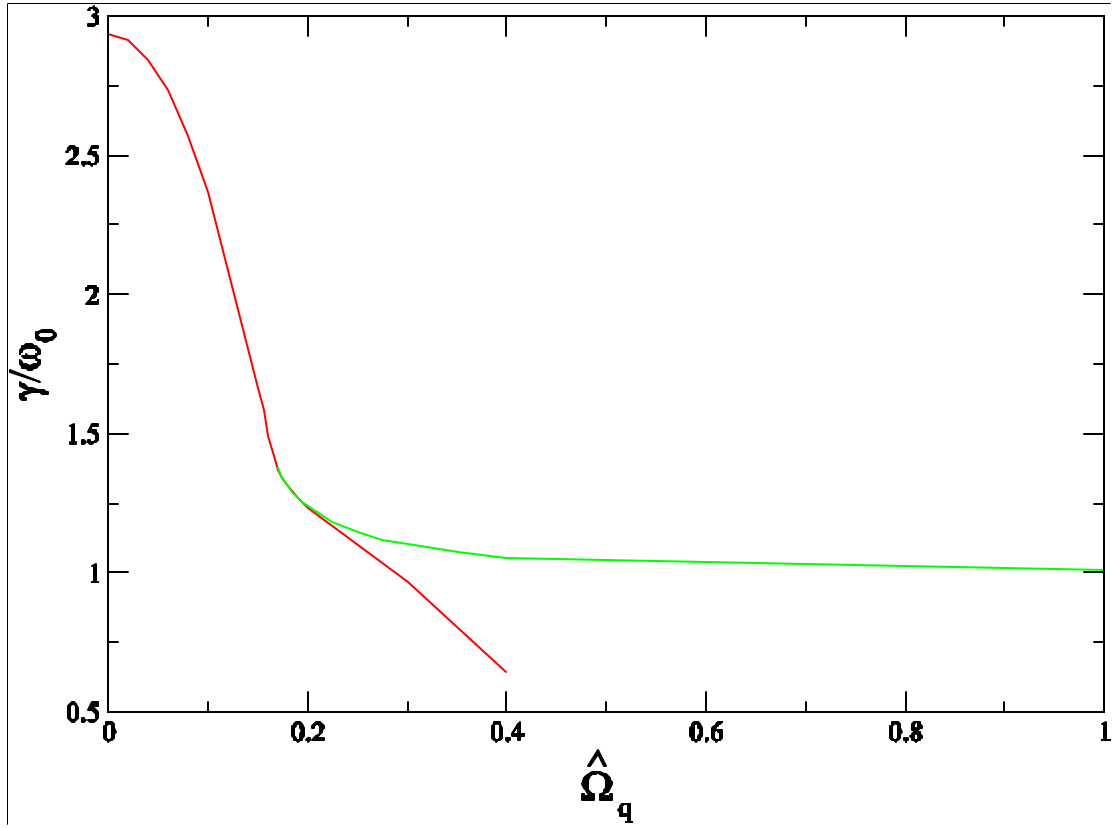


Fig. 3: The variation of the normalised growth rate, γ/ω_0 , with increasing flow shear, $\hat{\Omega}_q$, for the lowest conventional ballooning mode harmonic, $p = 0$, for the case with only a radial profile for the growth rate: $\Lambda_0^2 = 15$, $\hat{\epsilon}_0 = 2$, $\alpha = d = 0$, $\gamma_0/\omega_0 = 1$.

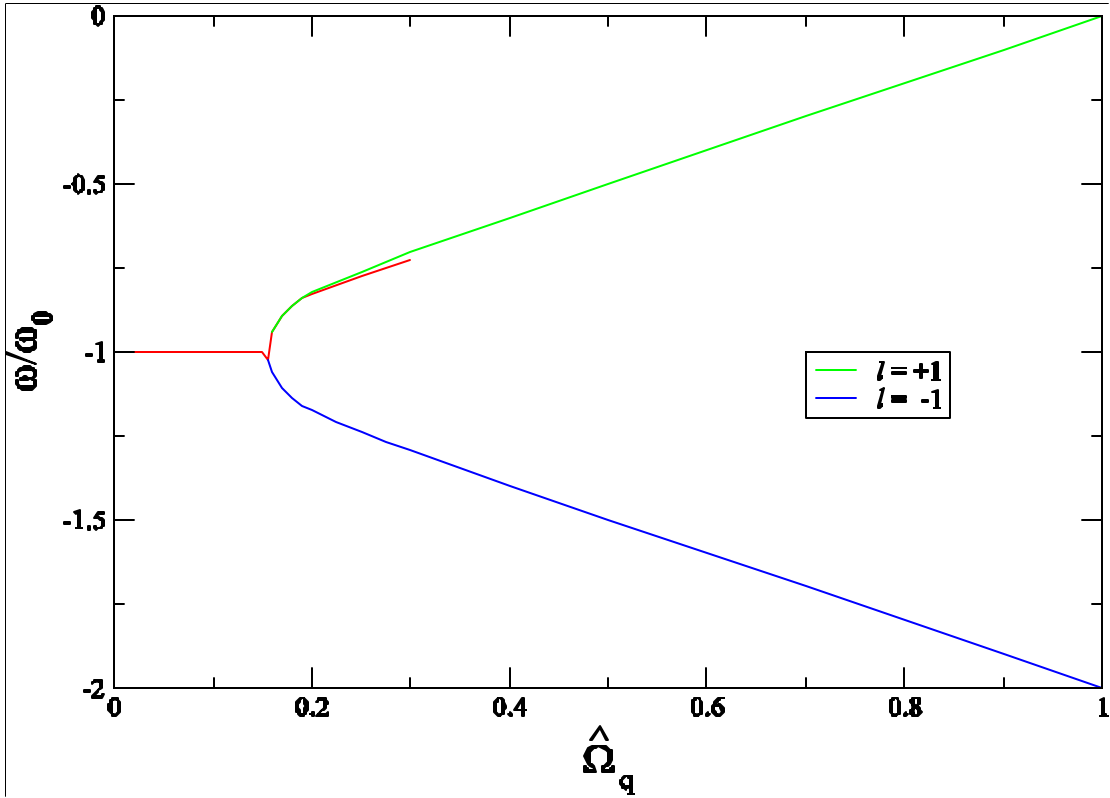


Fig. 4: The variation of normalised frequencies, ω/ω_0 , with $\hat{\Omega}_q$ for the $p = 1$ and 2 harmonics for the case in Fig. 3, showing a coalescence of the two roots and the onset of two real frequencies.

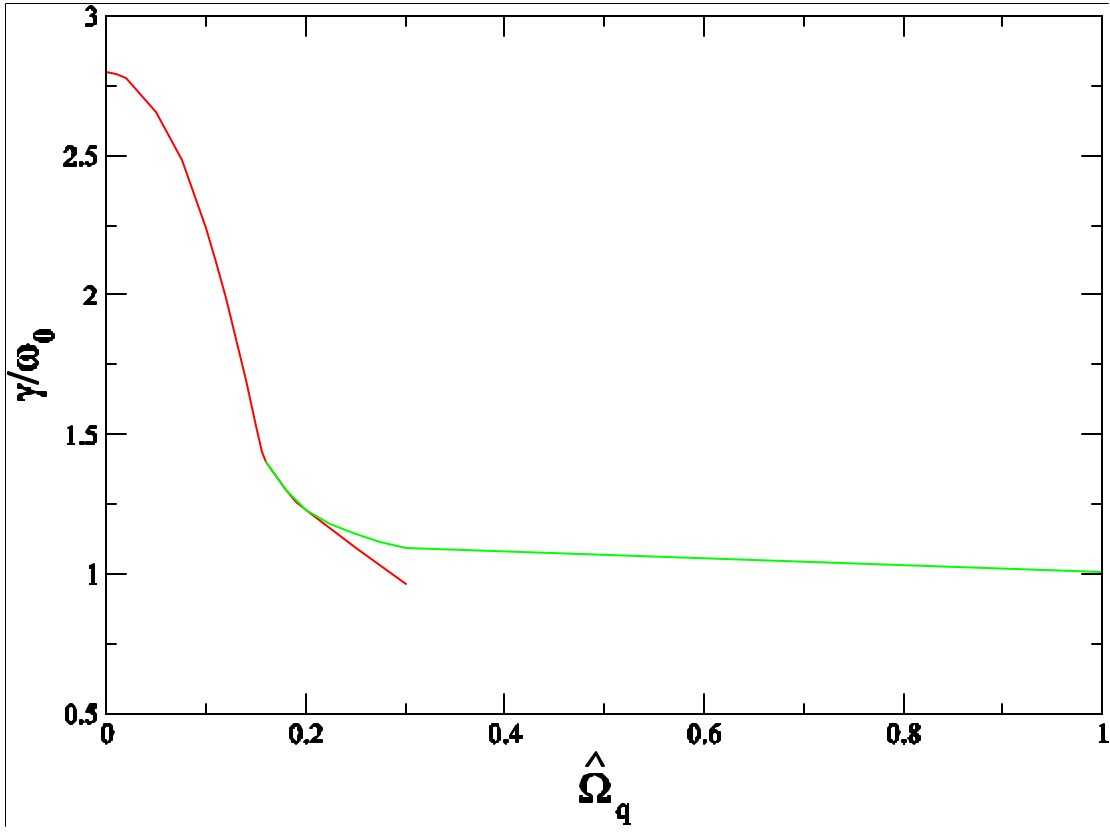


Fig. 5: As for Fig. 3, but for the next two harmonic, $p = 1$.

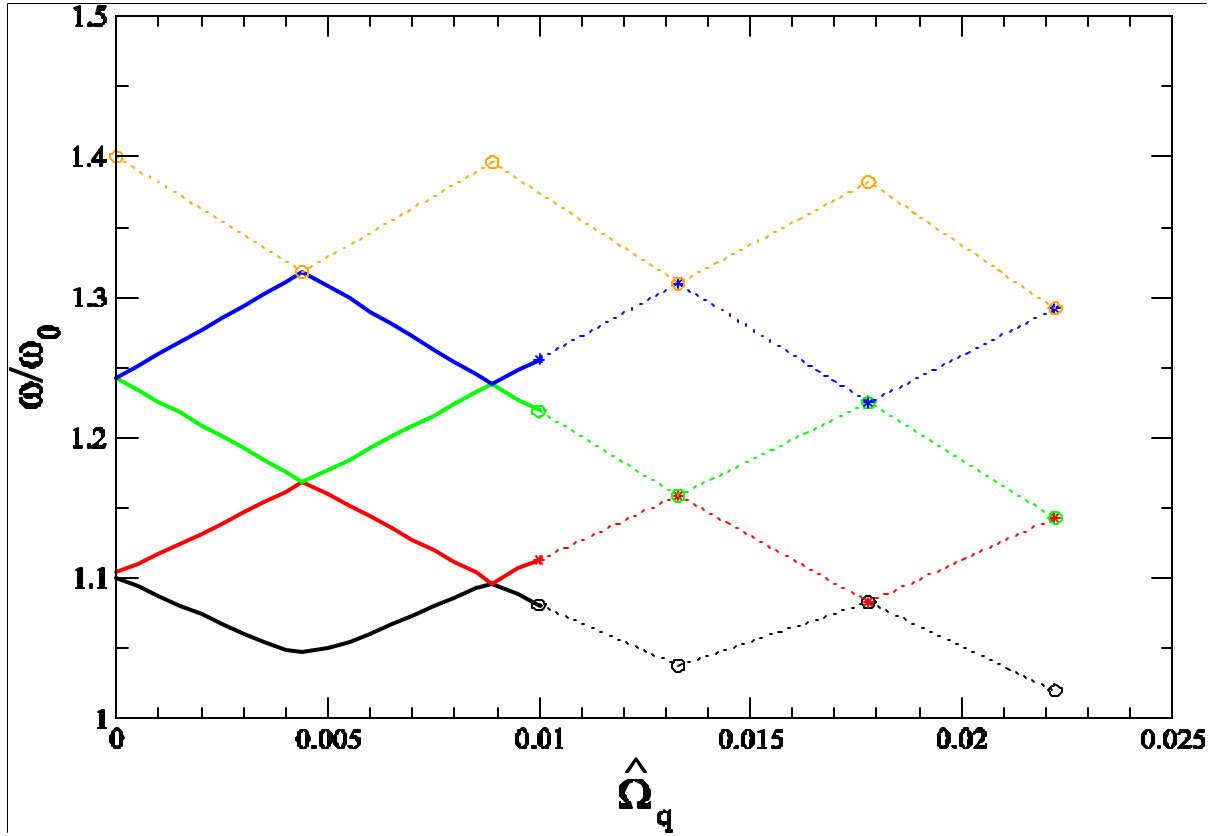


Fig. 6: The variation of the frequencies of some of the lowest passing harmonics of the conventional ballooning mode as $\hat{\Omega}_q$ increases for the case when there is only a radial variation of the real frequency: $\Lambda_0^2 = 15$, $\hat{\epsilon}_0 = 2$, $\alpha = p/4$, $d = -p/2$, $\gamma_0/\omega_0 = 1$. The full lines are complete calculations, the dashed lines are merely indicative, but do join computed minima and maxima of roots. One sees multiple coalescences.